Suppression of ISI Caused by Sampling Time Offset in IFDMA Systems

Alexander Arkhipov, Michael Schnell
German Aerospace Center (DLR), Inst. of Communications and Navigation, D-82234, Wessling, Germany.
Phone/e-mail: +49-8153-282873/firstname.lastname@dlr.de

***Abstract*— In this article, we investigate the influence of sampling time offset on the bit error rate (BER) performance in interleaved frequency-division multiple-access (IFDMA) uplink systems. It is shown that even small sampling time offset results in inter-symbol interference (ISI) and in signal-to-noise ratio (SNR) degradation. To avoid this, a soft ISI suppression algorithm is proposed which allows to significantly improve the system performance. The proposed algorithm can be applied to both IFDMA uplink systems and to conventional orthogonal frequency-division multiple-access (OFDMA) uplink systems.**

I. Introduction

Recently, IFDMA attained significant importance and is considered as an air interface candidate for 4G mobile communications [1] [2]. IFDMA is equivalent to an OFDMA-CDM [3] scheme with block interleaved frequency allocation and Fourier spreading [4] [5]. Compared to conventional OFDMA [6], IFDMA seems more attractive due to its lower complexity, since IFDMA requires no discrete Fourier transform (DFT) at the transmitter. Moreover, IFDMA shows a significantly lower peak-to-average power ratio (PAPR) than conventional OFDMA.

In a real IFDMA uplink system, sampling time offsets and frequency offsets are different for different users. Frequency offsets occur because of a non-zero relative speed between a base station and mobile terminals or because of slightly different oscillator frequencies at the receiver and the transmitter. Frequency offset estimation in IFDMA systems is out of the scope of this article and is considered in [7].

IFDMA system with rectangular pulse-shaping exhibits an inefficient power density spectrum [8]. Application of a pulse-shaping filter with acceptable spectral characteristics reduces excess bandwidth, but such an IFDMA system requires fine synchronization in time. If pulse-shaping is applied, the problem of correct sampling arises [8]. Sampling time offset results in SNR degradation and ISI. Both these effects lead to the performance degradation in IFDMA systems. In addition, different users have different sampling time offsets which makes the problem of sampling time offset estimation more difficult. In this contribution, it is shown that ISI is responsible for the main part of IFDMA system performance degradation, especially if the sampling time offset is large.

In this contribution, we propose a soft algorithm for ISI suppression. The algorithm estimates the reliability of received code bits, reconstructs and eliminates the ISI. Since soft values are used, the quality of the ISI reconstruction can be enhanced substantially. The proposed algorithm requires an estimate of the sampling time offset. Such an estimate can be obtained by performing an oversampling at the receiver as described in [8].

We use the following notation: variables denoting signals in time domain are written in small letters, variables denoting signals in frequency domain are written in capital letters. Bold variables designate matrices or vectors.

The remainder of the paper is organized as follows. Section II introduces the IFDMA scheme. In Section III, the influence of sampling time offset on the system performance is studied. Section IV describes the proposed algorithm for soft ISI suppression. Simulation results are discussed in Section V. Finally, Section VI concludes the paper.

II. Interleaved Frequency-Division Multiple Access (IFDMA) Scheme

In the following, IFDMA is described as a special case of OFDMA-CDM. For additional descriptions of the IFDMA scheme refer to [4] [9]. The standard OFDMA-CDM [3] uplink transmission system is able to support up to K simultaneously active users. Assume that N_u users ($N_u \leq K$) transmit simultaneously. Each OFDMA-CDM user $i = 0, \ldots, N_u$, performs a blocked transmission of Q complex-valued symbols $d_q^{(i)}, q = 0, \ldots, Q-1$. Each symbol $d_q^{(i)}$ is obtained after the modulation of the qth independent data stream coming from the qth channel encoder as shown in Fig. 1. Such a coding scheme allows an iterative interference cancellation scheme, as described in [3], and is used for the ISI suppression in this contribution. The average energy of the transmitted data symbol $d_q^{(i)}$ is unity and the symbol duration is T_s. The Q symbols are arranged to build the symbol vector $\mathbf{d}^{(i)}$ of user i

$$\mathbf{d}^{(i)} = (d_0^{(i)}, d_2^{(i)}, \ldots, d_{Q-1}^{(i)}). \tag{1}$$

The symbol vector $\mathbf{d}^{(i)}$ is first serial-to-parallel converted. Then, a code-division multiplexing (CDM) component is introduced by spreading each symbol with a different spreading code $\mathbf{c}_q, q = 1, \ldots, Q$, of length $L \geq Q$ and adding together the resulting Q spread symbols. After summation, the resulting vector $\mathbf{s}^{(i)}$ can be represented by

$$s_n^{(i)} = \sum_{q=1}^{Q} c_{n,q} \cdot d_q^{(i)}, n = 0, \ldots, L-1, \tag{2}$$

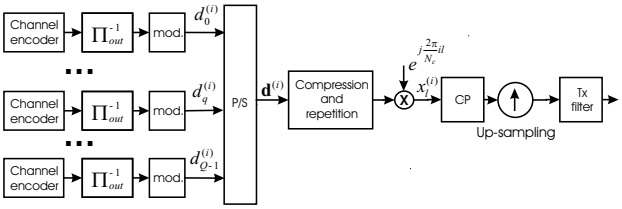

Fig. 1. The IFDMA transmitter for user i

where $c_{n,q}$ is the n-th component of the spreading code $\mathbf{c}_q$, $q = 0, \ldots, Q-1$. Finally, an inverse DFT (IDFT) with user-specific frequency mapping is performed for the row vector $\mathbf{s}^{(i)}$. Block interleaving achieves optimal frequency diversity, since it distributes the L spread symbols of the Q data symbols of user i equally over the whole transmission bandwidth. Note, OFDMA-CDM exclusively assigns to each of the K users a set of L frequencies out of all possible $N_c = KL$ subcarriers. If all subcarriers assigned to user i are uniformly spaced over the whole available transmission bandwidth at a distance N_c/K, the time domain transmit signal $x_l^{(i)}, l = 0, \ldots N_c-1$, obtained after the IDFT operation in the transmitter, can be represented by

$$x_l^{(i)} = e^{j\frac{2\pi}{N_c}il} \frac{1}{\sqrt{N_c}} \sum_{n=0}^{L-1} s_n^{(i)} e^{j\frac{2\pi}{L}nl}. \tag{3}$$

As in standard OFDMA, a guard interval larger than the maximum channel delay is added as a cyclic prefix (CP) in OFDMA-CDM in order to avoid interference from preceding OFDMA-CDM transmission symbols.

IFDMA as a special case of OFDMA-CDM can be realized if a fully loaded system, i.e. $L = Q$, is considered and Fourier codes with components $c_{n,q} = \{e^{-j\frac{2\pi}{Q}nq}\}, n = 0, \ldots, L-1, q = 0, \ldots, Q-1$, are used for spreading. In this case, the Fourier codes for spreading and the rotation factors of the Fourier transform cancel out and the transmit signal given in (3) reduces to

$$x_l^{(i)} = \underbrace{e^{\frac{j2\pi}{N_c}il}}_{\text{user specific phase factor}} \cdot \underbrace{\frac{1}{\sqrt{K}} d_{l \bmod L}^{(i)}}_{\text{transmitted chips}}, l = 0, \ldots, N_c - 1. \tag{4}$$

Comparing (4) and [10] [9] it follows that IFDMA is equivalent to OFDMA-CDM with block interleaved frequency allocation and can be completely generated in the time domain without using the Fourier transform. The time domain generation of IFDMA uses compression and repetition as described in detail in [9]. Note, the multiplication with the user specific phase factor in (4) ensures the user discrimination by assigning to each user i a set of subcarriers orthogonal to all other users' subcarrier sets. Each sample $x_l^{(i)}$ represents the transmitting chip $l, l = 0, \ldots, N_c - 1$. The duration of the resulting chips is $T_c = T_s/K$.

The simulation model for the IFDMA is shown in Fig. 1. After addition of CP, the obtained signal is up-sampled. This up-sampling is implemented by adding zero samples between successive samples $x_l^{(i)}$. After up-sampling, the pulse-shaping is performed by a transmit filter. After analog-to-digital (A/D) conversion, we assume transmission over a time-dispersive mobile radio channel. At the receiver, we consider an oversampling per transmitted chip $x_l^{(i)}$. After sampling, signal is filtered by a receive filter, which is matched to the transmit pulse-shaping filter. In Fig. 2, the IFDMA signal after the receive filter is represented, with a 'dotted' line. In the down-sampling operation one sample per transmitted chip is chosen for equalization, despreading and estimation of the transmitted data.

For the sake of simplicity, the convolution of the receive and transmit filters is represented by a sampled function $g(t)$. In the following, function $g(t)$ is a Nyquist pulse

$$g(t) = \text{sinc}\left(\frac{t}{T_c}\right) \frac{\cos(\pi\alpha t/T_c)}{1 - 4\alpha^2 t^2/T_c^2}, \tag{5}$$

where α denotes the roll-off factor.

For the sake of simplicity, only one received sample y_l per transmitted chip $x_l^{(i)}$ is considered in the following. Therefore, we assume that channel has an impulse response described by a vector $\mathbf{h}^{(i)}$ of dimension M with components $h_m^{(i)}, m = 1, \ldots, M$.

Assume that value y_l represents the lth element of received vector $\mathbf{y}$, which can be represented as

$$\mathbf{y} = \sum_{i=1}^{N_u} \hat{\mathbf{h}}^{(i)} \mathbf{z}^{(i)}(\tau^{(i)}) + \mathbf{n}, \tag{6}$$

where vector $\mathbf{n}$ denotes samples of additive white Gaussian noise (AWGN). The channel matrix $\hat{\mathbf{h}}^{(i)}$

$$\hat{\mathbf{h}}^{(i)} = \begin{pmatrix} h_1^{(i)} & \cdots & h_M^{(i)} & 0 & \cdots & 0 \\ 0 & h_1^{(i)} & \cdots & h_M^{(i)} & \cdots & 0 \\ \vdots & \vdots & \ddots & \vdots & \vdots & \vdots \\ 0 & \ldots & h_1^{(i)} & \ldots & h_M^{(i)} & 0 \\ 0 & 0 & \ldots & h_1^{(i)} & \ldots & h_M^{(i)} \end{pmatrix} \tag{7}$$

is the $N_c \times N_c$ right circular matrix whose rows are cyclically shifted versions of the vector $\tilde{\mathbf{h}}^{(i)}$. The vector $\tilde{\mathbf{h}}^{(i)}$ is obtained by appending $N_c - M$ zeros to $\mathbf{h}^{(i)}$.

The elements $z_l^{(i)}(\tau^{(i)})$ of the vector $\mathbf{z}^{(i)}(\tau^{(i)})$ in (6) can be represented as

$$z_l^{(i)}(\tau^{(i)}) = e^{j\frac{2\pi}{N_c}i(l+\frac{\tau^{(i)}}{T_c})} \frac{1}{\sqrt{K}} \cdot \left[d_{l \bmod L}^{(i)} g\Big(\tau^{(i)}\Big) + \underbrace{\sum_{\substack{p=0 \\ p \neq l}}^{N_c-1} d_{p \bmod L}^{(i)} g\Big(\tau^{(i)} + (p-l)T_c\Big)}_{\text{ISI}} \right]. \tag{8}$$

The normalized time offset $\tau^{(i)}$ can take on values in the range $-T_c/2 \leq \tau^{(i)} \leq T_c/2$. The orthogonality between users is not violated since $\tau^{(i)}$ does not introduce any frequency offset. However, ISI appears if a sampling time offset $\tau^{(i)}$ is present

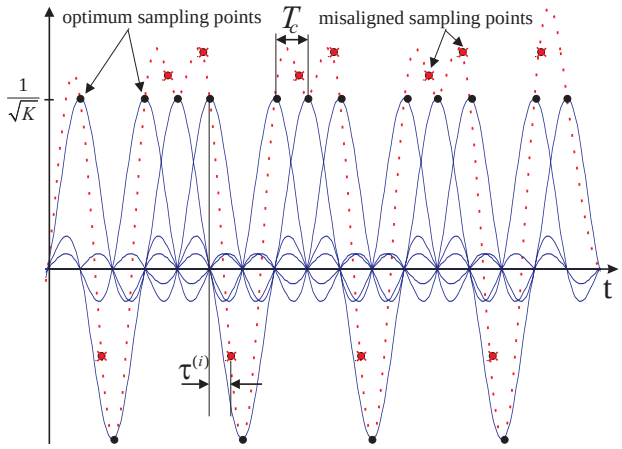

Fig. 2. Example of the IFDMA signal after the receive filter. Sampling time offset $\tau^{(i)}$ causes SNR degradation and leads to the ISI; $\mathbf{d}^{(i)} = [1,-1,1,1]^T$; $L = Q = 4$; $\alpha = 0.25$; only user $i = 0$ is active; AWGN channel with a negligible noise power.

as shown in Fig. 2. The optimum sampling points correspond to a situation where $\tau^{(i)} = 0$. In this case, the received signal $\mathbf{y}$ of user i is ISI-free.
Other users transmit their data on separated orthogonal subcarriers and their influence is not considered in the following. Thus, we omit subscript i for simplicity, and focus on the data of user i.

III. ISI AND SNR DEGRADATION DUE TO THE SAMPLING TIME OFFSET

We consider vector $\mathbf{z}(\tau)$ in our analysis of ISI. ISI appears if a sampling time offset τ is present as shown in (8). If L is large enough, the variance of the ISI for chip x_l can be approximated as

$$\sigma^2_{\text{ISI}}(\tau) = \frac{1}{K} \sum_{\substack{p=0 \\ p \neq l}}^{N_c-1} g^2(\tau + (p-l)T_c)\,. \tag{9}$$

If operator $E\{.\}$ denotes the expectation, the energy of the useful signal in (8) decreases with τ according to

$$E\{|d_{l \bmod L} g(\tau)|^2\}/K = g^2(\tau)/K. \tag{10}$$

Additional phase rotation in (8) can be mitigated by a channel estimation algorithm and does not have any negative impact on the system performance.

IV. SOFT ISI SUPPRESSION

The soft ISI suppression scheme for the symbol $d_q, q = 0,\ldots,Q-1$ is shown in Fig. 3. It is assumed that a main part of the ISI comes from the symbol $d_{(q-1) \bmod Q}$ and the symbol $d_{(q+1) \bmod Q}$. A reconstruction of the ISI is performed in the upper part, whereas the final decoding of a data stream corresponding to the data symbol d_q is done in the lower part. A reconstruction of the ISI is performed as follows. The received time domain signal $\mathbf{y}$ is converted into frequency domain, by applying a DFT of length N_c. The obtained frequency domain vector $\mathbf{Y}$ is then frequency demapped. The frequency demapping assumes that only the subcarriers $\kappa = nK+i, n = 0,\ldots,L-1$ are taken for despreading. After despreading, the equalization is performed. In the following, a minimum mean square (MMSE) equalization technique is considered [3]. Despreaidng assumes a multiplication by a code, which is complex conjugate to the code $\mathbf{c}_{(q-1) \bmod Q}$. After symbol demapping and deinterleaving, the log-likelihood ratio (LLR) of received bits is calculated as described in [11]. The output of the LLR block is the LLR value $\lambda^{(j-1)}_{(q-1) \bmod Q}$ for each coded bit, where $j = 1,\ldots,J$ designates the iteration number and J denotes the total number of iteration. Values $\lambda^{(0)}_{(q-1) \bmod Q}$ denote LLR values of bits corresponding to the data stream $(q-1) \bmod Q$ obtained after the initial iteration. The soft in/out channel decoder performs maximum a posteriori probability estimation for code bits [11]. Thus, the output of this decoder are re-encoded log-likelihood values LLR_{re}. These values are calculated for each code bit.
The soft bit value w [12] is defined as

$$w = \tanh\{LLR_{\text{re}}/2\}. \tag{11}$$

The soft bit w can take on values in the interval [-1,1]. Note that we omitted index q in (11). After the soft symbol mapping, compression and repetition is performed as described in the previous section. Multiplication with the vector $\mathbf{u}$ assures a correct weighting of the obtained ISI. The elements $u_l, l = 0,\ldots,N_c-1$ of the vector $\mathbf{u}$ are defined as

$$u_l = \frac{1}{\sqrt{K}} g(T_c+\tau) e^{j\frac{2\pi}{N_c} i(l+\frac{\tau}{T_c}+1)}. \tag{12}$$

A convolution with the channel impulse response $\mathbf{h}$ is realized by a multiplication with the channel matrix $\hat{\mathbf{h}}$. However, this convolution can be efficiently realized by using only two DFT operations and one vector multiplication.
The reconstructed ISI of the symbol $d_{(q-1) \bmod Q}$ is subtracted from the frequency-domain signal $\mathbf{Y}$.
The following remarks are of interest:

- Proposed soft ISI suppression scheme requires an estimation of the sampling time offset τ. This estimation can be performed as described in [8].
- The ISI coming from the data symbol $d_{(q+1) \bmod Q}$ must also be reconstructed and subtracted. A reconstruction of the ISI is performed exactly in the same way as for the data symbol $d_{(q-1) \bmod Q}$, only the sign of τ must be changed in (12).
- For small values of the roll-off factor α in (5) or for large values of τ, the subtraction of ISI coming from only one preceding and only one following data symbol is not enough. In this case, the performance of the considered system can be improved if the ISI from other interfering symbols is subtracted as well.
- Multiple iterations can improve the performance of the soft ISI suppression algorithm significantly. Obtained values $\lambda^{(j)}_q, q = 0,\ldots,Q-1$ can be used in succeeding iterations as input of the soft in/out decoder.

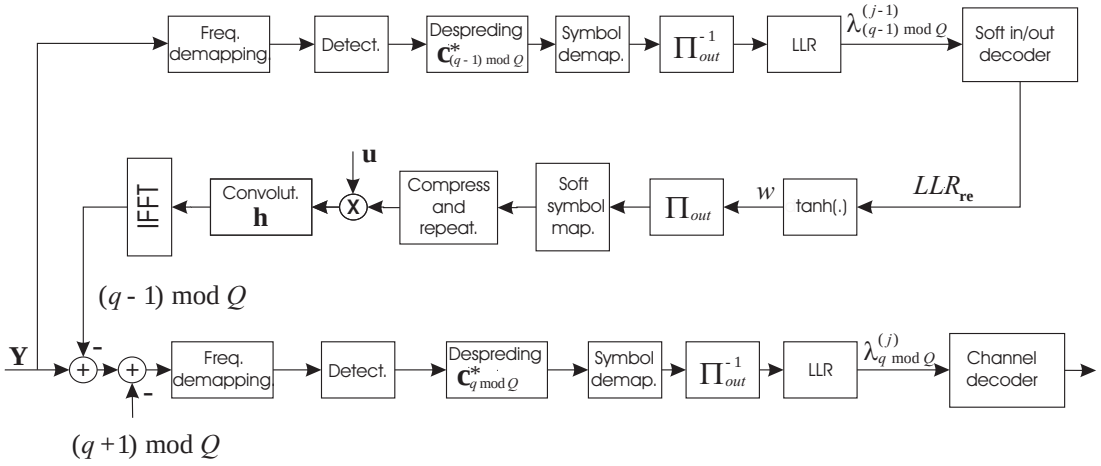

Fig. 3. Iterative scheme for the ISI suppression for symbol $d_q, q = 0, \ldots, Q-1$

V. Simulation Results

The transmission system has a bandwidth of 20 MHz and the carrier frequency is 5 GHz. The number of subcarriers is $N_c = 1024$. The spreading length is $L = 64$ and the maximal number of users is $K = 16$. A convolutional code with rate $1/2$ and memory 6 is used in our simulations. The frame consists of 24 IFDMA symbols. QPSK modulation alphabet is used. The roll-off factor α changes from 0.25 to 0.75. Influence of the received and the transmit filter is modelled by the function $g(t)$, which is non-zero only in the range $-3T_c < t < 3T_c$. Therefore, if sampling time offset occurs, each transmitted chip x_l experiences ISI from three preceding and three following chips.

A multipath channel model is considered, which consists of a tapped delay line with $M = 11$ statistically independent Rayleigh fading taps. The average power for each channel component $h_m, m = 1, \ldots, M$, is modelled as

$$E\{|h_m|^2\} = -m + 1 \text{ (dB)}. \tag{13}$$

Additionally, the average channel attenuation is normalized to unity in our simulations. It is known, that system performance depends on the channel diversity. If we increase a mobile terminal speed the system performance improves, since channels gets more time diversity. Two different mobile terminal speeds are considered. The first one is equal to 0 km/h and corresponds to a slowly changing mobile channel, whereas the second one is equal to 250 km/h and corresponds to the fast changing mobile channel.

The bit error rate (BER) curves versus SNR are presented in Fig. 4 for the case of $\tau = \frac{4}{18}T_c$, $\tau = \frac{7}{18}T_c$ and slowly changing channel. As a reference, the curve for the case $\tau = 0$ is shown. It is seen that the system performance degrades if τ increases. The solid line curves in Fig. 4 denote the system performance with a MMSE detector . The dotted lines denote lower bounds which are obtained by shifting the reference curves to the right. This shift is calculated from (10) and represents the SNR degradation due to the sampling time offset τ. For the BER equal to 10^{-3} and $\tau = \frac{7}{18}T_c$ a performance gap between the lower bound curve and the MMSE curve is about 8.5 dB. For $\tau = \frac{4}{18}T_c$, the performance degradation is about 2dB.

The dashed line represents performance of the ISI suppression algorithm. For the case $\tau = \frac{4}{18}T_c$, the lower bound can be reached. For $\tau = \frac{7}{18}T_c$, the BER performance can be improved approximately by 6.5 dB. However, the performance gap between the lower bound curve and the dashed curve is still about 2 dB. The problem is that ISI from one successive and one following symbol is subtracted in Fig. 4. The residual ISI stems from other data symbols and this ISI is partly responsible for the remaining performance gap of 2 dB.

The suppression of the residual ISI is thoroughly investigated in Fig. 5. Two different sets of curves are simulated for two different speeds of mobile terminals in order to illustrate the performance of the ISI suppression algorithm in dependance on a channel diversity. In each simulation set two cases are considered. In the first case, the ISI coming from one successive and one following data symbol is subtracted only, i.e the ISI from $d_{(q-1) \bmod Q}$ and $d_{(q+1) \bmod Q}$. The curves corresponding to this case are marked as '1 symbol' in Fig. 5. The case '2 symbols' corresponds to a situation, where ISI coming from the data symbols $d_{(q-1) \bmod Q}$, $d_{(q+1) \bmod Q}$, $d_{(q-2) \bmod Q}$ and $d_{(q+2) \bmod Q}$ is subtracted. As a reference, the lower bound curve for the fast changing channel and $\tau = 0$ is depicted in Fig. 5.

It is seen that additional subtraction of the ISI coming from $d_{(q-2) \bmod Q}$ and $d_{(q+2) \bmod Q}$ improves the BER performnce. However, this performance gain is about 1 dB for the slowly changing channel. It is seen that the BER system performance improves if we increase channel diversity. However, this improvement is of a minor importance. It is seen that the performance gap between the lower bound and the case of ISI suppression with two symbols is still about 2 dB. This effect can be explained as follows.

At the high values of sampling time offset, e.g., $\tau = \frac{7}{18}T_c$, the SNR degrades and ISI increases drastically. Thus, the prob-

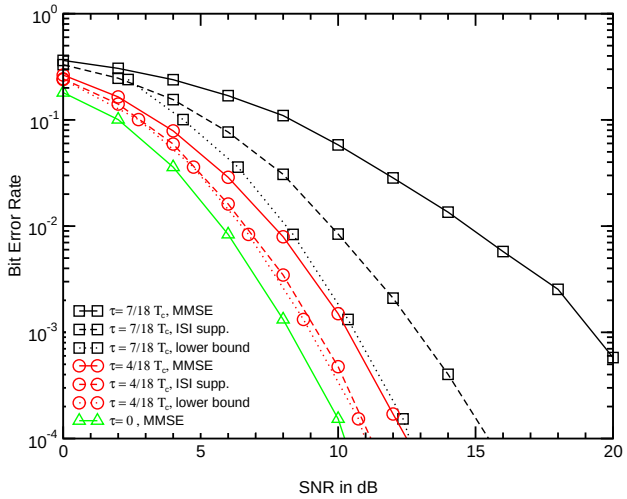

Fig. 4. The BER performance versus SNR for different values of sampling time offset τ; IFDMA system with the soft ISI suppression algorithm; 1 iteration; slowly changing channel

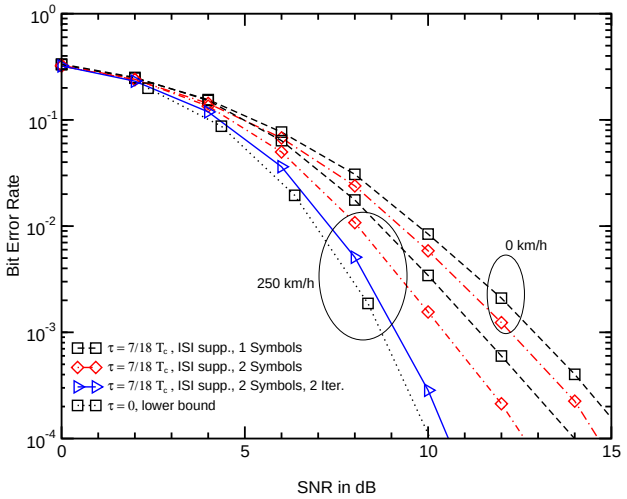

Fig. 5. The BER performance versus SNR for a different number of subtracted interfering symbols and different number of iterations; IFDMA system with the soft ISI suppression algorithm

ability to distinguish between two neighboring data symbols decreases. Moreover, two neighboring data symbols experience exactly the same influence of the transmission channel, e.g., can be deeply faded. If this situation, the probability to reconstruct the ISI correctly decreases tremendously. Thus, the quality of the reconstructed ISI decreases and, as a result, some residual ISI remains. In this instance, data stream with subtracted ISI cannot be decoded perfectly since this data stream experiences exactly the same bad channel condition. The logical countermeasure can be to use multiple iterations in the ISI suppression algorithm.

This performance of the ISI suppression algorithm with multiple iterations is shown in Fig. 5. This results verifies our approach. If sampling time offset τ is large it is useful to apply multiple iterations in order to improve the IFDMA system performance. Only one additional iteration allows to improve the system performance by 1.5 dB and closely approach the lower bound.

VI. Conclusions

The ISI appears because of the sampling time offset which causes remarkable performance degradation. A time offset equal to the one half of the chip duration makes successful data transmission impossible. In this contribution, we propose the efficient algorithm for the soft ISI suppression. The proposed algorithm allows to achieve an optimum performance and completely eliminate the ISI for the small values of the sampling time offset. For large values of sampling time offset, the performance improvement is significant and the IFDMA system performance can reach the lower bound at the price of a high complexity.

Acknowledgments

The work presented in this paper is carried out in the framework of the 4MORE (4G MC-CDMA multiple antenna system On chip for Radio Enhancements) project [2], which is supported by the European Commission within FP6 under the contract number IST-2002-507039. The authors would like to acknowledge this support and this opportunity to conduct the research work.

References

[1] H. Atarashi and M. Sawahashi, "Broadband wireless access based on VSF-OFCDM and VSCRF-CDMA and its experiments", *In Proc. Multi-Carrier Spread Spectrum & Related Topics (MC-SS)*, Sept. 2003.

[2] IST 4MORE project, web site http://www.ist-4more.org.

[3] S. Kaiser, "OFDM code division multiplexing in fading channels", *IEEE Transactions on Communications*, vol. 50, no. 8, pp. 1266–1273, Aug. 2002.

[4] A. Arkhipov and M.Schnell, "Interleaved frequency-division multiple-access system with frequency domain equalization", *International OFDM Workshop 2004, Dresden, Germany*, Sep. 2004.

[5] K. Bruninghaus and H. Rohling, "Multi-carrier spread-spectrum and its relation to single-carrier transmission", *In Proc. of the IEEE VTC'98, Ottawa, Canada*, 1998.

[6] R.V. Nee and R. Prasad, *OFDMA for Wireless Multimedia Communications*, Artech House, 2002.

[7] A. Arkhipov and M. Schnell, "Frequency offset estimation for IFDMA uplink systems", *IEEE GLOBECOM'06, San Francisco, California, USA*, Nov. 2006.

[8] A. Arkhipov and M.Schnell, "Sampling time offset estimation for IFDMA uplink systems", *IEEE International Conference on Communications (ICC 2007)*, Submitted.

[9] M. Schnell, I. De Broeck, and U. Sorger, "A promising new wideband multiple-access scheme for future mobile communications systems", *European Transactions on Telecommunications (ETT)*, vol. 10, No. 4, pp. 417–427, Jul./Aug. 1999.

[10] U. Sorger, I.De Broeck, and M. Schnell, "Interleaved FDMA - a new spread-spectrum multiple-access scheme", *In Proc. of IEEE International Conference on Communications (ICC'98)*, pp. 1013–1017, June.1998.

[11] J. Proakis, *Digital Communications*, McGraw Hill Higher Education, Dec. 2000.

[12] S. Kaiser, *Multi-Carrier CDMA Mobile Radio Systems - Analysis and Optimization of Detection, Decoding and Channel Estimation*, Düsseldorf: VDI Verlag, Fortschritt-Berichte VDI, series 10, no. 531, 1998.